Journal of Cell Science 107, 105-115 (1994)
Printed in Great Britain © The Company of Biologists Limited 1994
JCS6620

Intracellular distribution of β-actin mRNA is polarized in embryonic corneal epithelia

Berhan Yeh and Kathy Kay Hartford Svoboda*

Department of Anatomy and Neurobiology, Boston University School of Medicine, 80 East Concord St, Boston, MA 02118, USA

*Author for correspondence

SUMMARY

The intracellular distribution of filamentous actin (F-actin), all actin isoforms and β-actin mRNA were analyzed in whole-mount preparations of freshly isolated corneal epithelia. Filamentous actin distribution was analyzed with fluorescently tagged phalloidin. An antibody that recognizes an epitope on both globular (G-actin) and F-actin was used in an immunohistochemical analysis of actin protein distribution. Whole-mount epithelial tissues were examined with a confocal laser scanning microscope (CLSM). Biotinylated oligonucleotide probes specific for the β-actin mRNA were used, and visualized with avidin-FITC. The intracellular localization of the β-actin mRNA was similar to the F-actin protein distribution. In the most apical optical sections of embryonic cornea, actin staining delineated the cell borders and microvilli of the periderm cells. The actin is also detected as an organized network at the interface between the basal and periderm cells. At the level of the basal cell nucleus, F-actin is sparse, associating only with the lateral cell membranes. However, at the optical plane below the nuclei, the actin forms an elaborate actin cortical mat. Actin mRNA staining was visualized as discrete punctate areas. The β-actin mRNA was positive at the optical plane just below the periderm cell apical membrane surface, similar to actin in microvilli. These cells also contained punctate staining near the cell membranes and in the periderm-basal cell junction area. At the level of the basal cell nucleus the actin mRNA was present in a punctate pattern along the cell membranes. Below the basal cell nuclei the actin mRNA staining increased at the level of the actin cortical mat. These experiments are the first demonstration that actin mRNA is polarized in embryonic corneal epithelia and co-localized with actin protein in an intact tissue.

Key words: actin, epithelial tissue, confocal microscopy, actin mRNA

INTRODUCTION

Actin mRNA is localized to the distal lamellapodia of cultured fibroblasts, myoblasts (Lawrence and Singer, 1986; Singer et al., 1986) and microvascular pericytes (Hoock et al., 1991). These regions have higher concentrations of actin and include polymerization sites for actin filament formation (Wang, 1984). Actin mRNA distribution in the intestinal epithelia has also been shown to parallel actin protein distribution in sectioned material (Cheng and Bjerknes, 1989). Recently, the translocation of actin mRNA to fibroblast lamellapodia has been shown to require intact microfilaments (Sundell and Singer, 1991), but is not dependent upon newly synthesized actin (Sundell and Singer, 1990).

Other investigators have reported that non-actin mRNA is also associated with the cytoskeleton. The hypothesis that active mRNA is associated with the cytoskeleton is supported by both morphological and biochemical evidence (Taneja et al., 1992). Polysomes have been seen in association with the cytoskeletal matrix in whole-mount preparations of cells (Wolosewick and Porter, 1976; Wolosewick and Porter, 1979), frozen fractured cells (Batten et al., 1980), and detergent-extracted cells (Lenk et al., 1977; Schliwa, 1982). The cytomatrix has been identified to contain predominantly actin. This was shown by labeling the actin with the S1 fraction of heavy meromysin (Batten et al., 1980; Schliwa, 1982), by two-dimensional gel electrophoresis (Schliwa, 1981) and by staining with [NBD]-phallacidin (Jeffery and Meier, 1983; Svoboda, 1992). In an independent study, actin mRNA and poly(A)$^+$ RNA are localized to the cytoskeletal framework of embryos by in situ hybridization, but histone mRNA is distributed throughout acidian eggs (Jeffery and Meier, 1983).

Independent biochemical studies demonstrate that in cells extracted with detergent, mRNA is localized to the non-soluble material or the 'cytoskeletal fraction' (CSK). This fraction contains microfilaments, intermediate filaments and stable microtubules (Ben-Ze'ev et al., 1979). The CSK also contains most of the polysomes and 70-80% of the poly(A)$^+$ mRNA (Lenk and Penman, 1979; Lenk et al., 1977). Perhaps the most conclusive evidence that mRNA is associated with actin is the ready extraction of mRNA from CSK by actin-disrupting drugs (Adams et al., 1983; Lenk and Penman, 1979; Ramaekers et al., 1983; Taneja et al., 1992). In addition, the translocation of actin mRNA in chick fibroblast cells decreases in the presence of cytochalasin D, an actin-disrupting drug, but not by

compounds that disrupt other cytoskeletal proteins (Sundell and Singer, 1991).

These studies on cultured fibroblasts have established some theories on spatial localization of specific mRNAs. The study on sectioned epithelial tissue using isotopic probes (Cheng and Bjerknes, 1989) provides limited information on cellular localization, but does not allow intracellular analysis of specific signals. In contrast, in situ hybridization using TEM techniques (Singer et al., 1989) allows subcellular localization of mRNA at the cost of losing the overall architecture of the tissue. To study an intact tissue such as the corneal epithelium, new methods were developed to determine the distribution of actin mRNA. We have used the confocal microscope to examine the distribution of actin protein and actin mRNA in primary whole tissues by optical sections. To accomplish this investigation it is important to recognize general morphological features from independent studies, such as TEM, SEM and/or video enhanced microscopy. Secondly, the tissue should then be re-examined with cytoarchitecture markers. The organelles should be located with specific stains. The specific proteins and mRNAs should be labeled with antibodies and probes (Svoboda, 1991, 1992).

The chick embryonic corneal epithelium has been well characterized as a two-cell layer structure with a thin flat outer layer, the periderm, and a cuboidal to columnar inner layer, the basal cells (Hay and Revel, 1969). The basal epithelial cells have a flat basal surface with a well-defined basal lamina (BL). Both cell layers are characterized by abundant secretory organelles necessary for the synthesis of the secreted glycoproteins that form the primary stroma (Hay and Revel, 1969; Hayashi et al., 1988). The purpose of this project is to examine the spatial relationship between the actin cytoskeleton and actin mRNA throughout both the periderm and basal cell layers.

We have previously shown that the actin cortical mat described from cross-sectional data obtained with electron micrographs (Meier and Hay, 1973; Svoboda and Hay, 1987; Hay and Svoboda, 1989) can be visualized by confocal microscopy (Svoboda, 1992). The confocal images actually show a wider distribution of actin microfilaments than the TEM cross-sections. The processing for TEM and the plastic embedding medium apparently destroys or hides many fine structures.

In the present investigation, confocal microscopy (CLSM) was employed to examine the spatial distribution of actin mRNA from freshly isolated corneal epithelia. These experiments show that the distribution of actin mRNA is extensive throughout both cell layers in a polarized distribution, with a remarkable co-distribution with actin protein.

MATERIALS AND METHODS

White Leghorn chicken eggs were obtained from SPAFAS (Norwich, CT) and incubated for 6 days at 38°C. Embryos were removed and rinsed in Hanks' balanced saline solution (HBSS). The whole corneas were removed from the embryos and incubated in Ca^{2+}/Mg^{2+}-free HBSS with 0.6 mg/ml dispase II (Boehringer Mannheim) for 1.5-3.0 minutes at 37°C. After the enzyme treatment, the whole corneas were rinsed in Ca^{2+}/Mg^{2+}-free HBSS. The epithelia were removed from the stroma using fine forceps with the basal lamina intact (+BL) and placed on black polycarbonate filters (0.4 μm pore size, Poretics).

Actin labeling

Actin is visualized with either fluorescently tagged phalloidin (Molecular Probes) or a monoclonal antibody, C4 (Lessard, 1988). The epithelia stained with phalloidin were fixed in PBS with 3.7% paraformaldehyde and 0.1% lysopalmitate (Svoboda, 1992). The whole corneas and epithelia were incubated in the phalloidin for 30-60 minutes at room temperature followed by 3× 10-minute rinses in PBS. The filters were placed epithelial side up in antifade mounting medium (Molecular Probes) on slides that had four nail-polish spacers, coverslipped, and viewed on a Leica confocal laser scanning microscope (CLSM).

The epithelia used for immunohistochemical identification of actin were fixed in acetone, blocked with 10% normal goat serum, and incubated in primary antibody (C4) overnight at room temperature (RT). After rinsing excess primary antibody, the tissue was incubated in secondary antibody (IgG H+L chains, Jackson Immunology) conjugated to FITC. The double-labeled epithelia were then incubated in rhodamine-phalloidin (Molecular Probes) for 30 minutes, rinsed and mounted onto slides as described previously.

Probe characteristics

The probes used for this study were human β-actin antisense and sense oligonucleotides (40mer, Oncogene Science). Oligonucleotide probes were 3′ end-labeled with terminal transferase (tdT, GIBCO-BRL) using either [^{32}P]dCTP or biotin-16-dATP as labels. The reaction was carried out in 50 μl with tdT buffer consisting of 25 μM of biotin-16-dATP (GIBCO-BRL), 140 mM potassium cacodylate, 30 mM Tris-HCl, pH 7.6, 1 mM DTT and 100 units of terminal transferase at 37°C for 3 hours. The reaction was stopped with 10 mM EDTA, ethanol precipitated, and resuspended in sterile water. The probes were divided into equal samples (135 ng/hybridization) each with 10 μg *E. coli* tRNA (Sigma) and 10 μg salmon sperm DNA (Sigma). This mixture was lyophilyzed and melted in 100% formamide (Sigma) at 90°C for 10 minutes before hybridization.

In situ hybridization

The complete in situ hybridization protocol has been previously described (Lawrence and Singer, 1986; Singer et al., 1986; Svoboda, 1991). Briefly, the isolated corneal epithelia were fixed with 4% paraformaldehyde/phosphate buffered saline (PBS)/5 mM $MgCl_2$, washed in PBS/5 mM $MgCl_2$, and stored in RNase-free 70% ethanol. All tissues were placed in 0.5 ml microtubes. The volume of incubations and rinses was enough to cover the tissues (50-100 μl).

Prior to hybridization the epithelia were rehydrated in 0.2 M Tris (pH 7.4), 0.1 M glycine for 10 minutes. Endogenous avidin and biotin sites were blocked (Vector Laboratories) at RT. The tissue was then equilibrated in 50% formamide, 2× SSC at 65°C for 15 minutes. The sodium chloride/sodium citrate (SSC) solution was 0.15 M NaCl, 0.015 M sodium citrate, pH 7.0. The formamide (Sigma) was deionized with mixed-bed resin beads, filtered and stored frozen.

The lyophilyzed probes were melted in formamide (10-30 μl). An equal volume of hybridization mix was added for a final concentration of 50% formamide, 2× SSC, 0.2% BSA, 10 mM vanadyl sulfate ribonucleoside complex (Bethesda Research Laboratories, BRL-GIBCO), 10% dextran sulfate (5′-3′) and 1 mg/ml each of *E. coli* tRNA and salmon sperm DNA. The final concentration of probe was 135 ng/50 μl hybridization (Singer et al., 1986; Svoboda, 1991). The epithelia were placed in sterile, 0.5 ml microtubes. The probe and hybridization mix were added, and then incubated at 37°C overnight in a thermocycler.

After hybridization, the tissue was washed with 2× SSC/50% formamide for 30 minutes at 37°C, then in 1× SSC/50% formamide for 30 minutes at 37°C, and then in 1× SSC, at RT twice for 30 minutes. Control 'blank' filters were incubated in the presence of ^{32}P-labeled probes and counted in the scintillation counter to determine the background from nonspecific sticking of the probe to the filters.

The preliminary experiments to determine optimal probe concentration and other hybridization parameters were conducted with ^{32}P-labeled probes. The hybridization of ^{32}P-labeled probe was determined by placing each epithelium in a scintillation vial, adding scintillation fluid (Econoflour, National Diagonstics), then counting the incorporation into the tissue. The samples for each treatment or probe (n=5) were averaged before further analysis. Once the optimum conditions were established, more epithelia were hybridized to biotin-labeled probes.

Avidin-FITC

After the unincorporated biotin-labeled probe was removed with repeated washes in 1× SSC, the cells were incubated in 4× SSC, 1% BSA for 10 minutes. The biotinylated probes were detected with avidin-FITC (Vector Laboratories) (2 μg/ml 4× SSC, 1% BSA) for 30 minutes, then washed 3 times in 2× SSC at RT on a rotating shaker (Belly Dancer). The tissue was then mounted in antifade mounting medium on slides, coverslipped and viewed on a Leica CLSM.

Controls

Some epithelia were incubated with RNase A (100 μg/ml in PBS for 1 hour at 37°C) to determine if the probes were specific for RNA. After incubation with RNase A, these epithelia were hybridized as described above with actin antisense oligonucleotides labeled with ^{32}P or biotin. After the washes, the ^{32}P-labeled epithelia were assessed by scintillation counting, and the biotin-labeled probes were incubated with avidin-FITC, then viewed by confocal microscopy.

A second type of control determined if the avidin was binding nonspecifically in the tissue. The tissue was incubated in the hybridization mixture without probe, washed, then reacted with FITC-avidin, washed and viewed with the confocal microscope.

The third control involved labeling the sense strand oligonucleotide to show that it did not hybridize above background levels with ^{32}P-labeled probes. Rat specific actin oligonucleotide probes were also used as a negative control. The fourth control was to place the empty black filters in the hybridization solution to determine the number of ^{32}P-labeled background counts as described above. Since the tissue is placed on these fluorescently negative (black) filters to maintain apical-basal polarity it is important to establish that the probe does not stick to the filters nonspecifically.

Confocal scanning microscopy

The specimens were analyzed with Leica upright confocal laser scanning microscope, CLSM, that is equipped with a argon ion laser with an output power of 2-50 mW, two photomultiplier tubes, and narrow band filters for double-labeling experiments. The apertures were set at the minimum size for optimal signal. Smaller apertures (pinhole) allow a narrower optical section and less background (Pawley, 1990; Wilson, 1990). The typical z-series is composed of optical sections in the xy optical plane. These images are en face optical sections through the vertical axis of the tissue. Each image of the series was taken at 1 μm intervals in the 512 × 512 pixel format. The objective lens used for the actin protein study was a ×50 water lens (NA 1.0). The objective lens used for the in situ hybridization study was a ×63 Plan apo oil lens (NA 1.4). The images were analyzed, enhanced and stored on an optical disc. Black and white photographs and pseudo color images were computer generated with a minimum of computer enhancement. These images were photographed with a 35 mm camera/50 mm lens on Kodak Ektachrome 100HC daylight or T-MAX 100 film. Cibachrome prints were made from color slides. All controls were collected, enhanced and photographed with the same conditions as the positive tissue.

Merged images were computer generated from two optical sections in the same focal plane recorded from the FITC or rhodamine photo multiplier tubes. The images were electronically colored so that the individual images were green and red. The combined image maintains the red or green color in pixels that do not overlap. Pixels that contain information from both images were colored yellow, indicating an overlap in the digital information.

RESULTS

General characteristics of the embryonic corneal epithelia

Unlike the adult corneal epithelium, the early chick embryonic epithelium is two cell layers thick, a thin flat outer layer, the periderm and a cuboidal basal cell layer (Fig. 1). The basal epithelial cells have a flat basal surface with a well-defined basal lamina (BL). Both of the cell layers are characterized by abundant secretory organelles, necessary for the synthesis of secreted glycoproteins that form the primary stroma (Hay and Revel, 1969; Hayashi et al., 1988). This has been illustrated in the cross-section diagram (Fig. 1). The chick corneal epithelium begins differentiation after the lens vesicle completely buds off on day 3. Endothelial cells migrate between the primary stroma and lens on day 5 of development. Then neural crest-derived fibroblast cells invade the primary stroma a day later and begin producing the secondary stroma (Hay and Revel, 1969). This drawing illustrates the cytoarchitecture of this early stage corneal epithelium (Fig. 1).

Before the complicated attachment system of hemidesmosomes and anchoring fibrils develops on day 10, the chick epithelial basal cell surface interacts with the underlying stroma by connections to the BL through ECM receptor molecules (Quaranta and Jones, 1991; Stepp et al., 1993; Sugrue, 1987, 1988; Sugrue and Hay, 1986). The basal area of the cell is rich in many cell organelles such as rough endoplasmic reticulum (RER), Golgi apparatus, secretory granules, mitochondria and organized cytoskeletal structures (Svoboda and Hay, 1987; Svoboda, 1992).

The periderm cells are large polygonal cells that can exceed 25 μm in diameter and 6-8 μm in width. These cells have F-actin in the microvilli and another actin network at the basal cell junction area (Svoboda, 1992). The basal cells of the

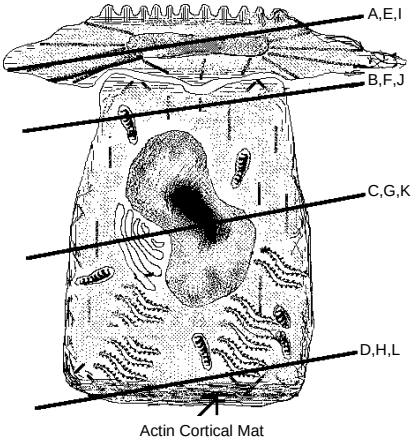

Fig. 1. Schematic drawing of the corneal epithelial cell. This cross-section drawing of the corneal epithelial cells shows the level of the four optical planes that correspond to the micrographs in Fig. 2. The fine lines represent actin, and thicker lines indicate the area of cytokeratin filaments. Other cell organelles, nuclei, mitochondria, Golgi and RER are also represented.

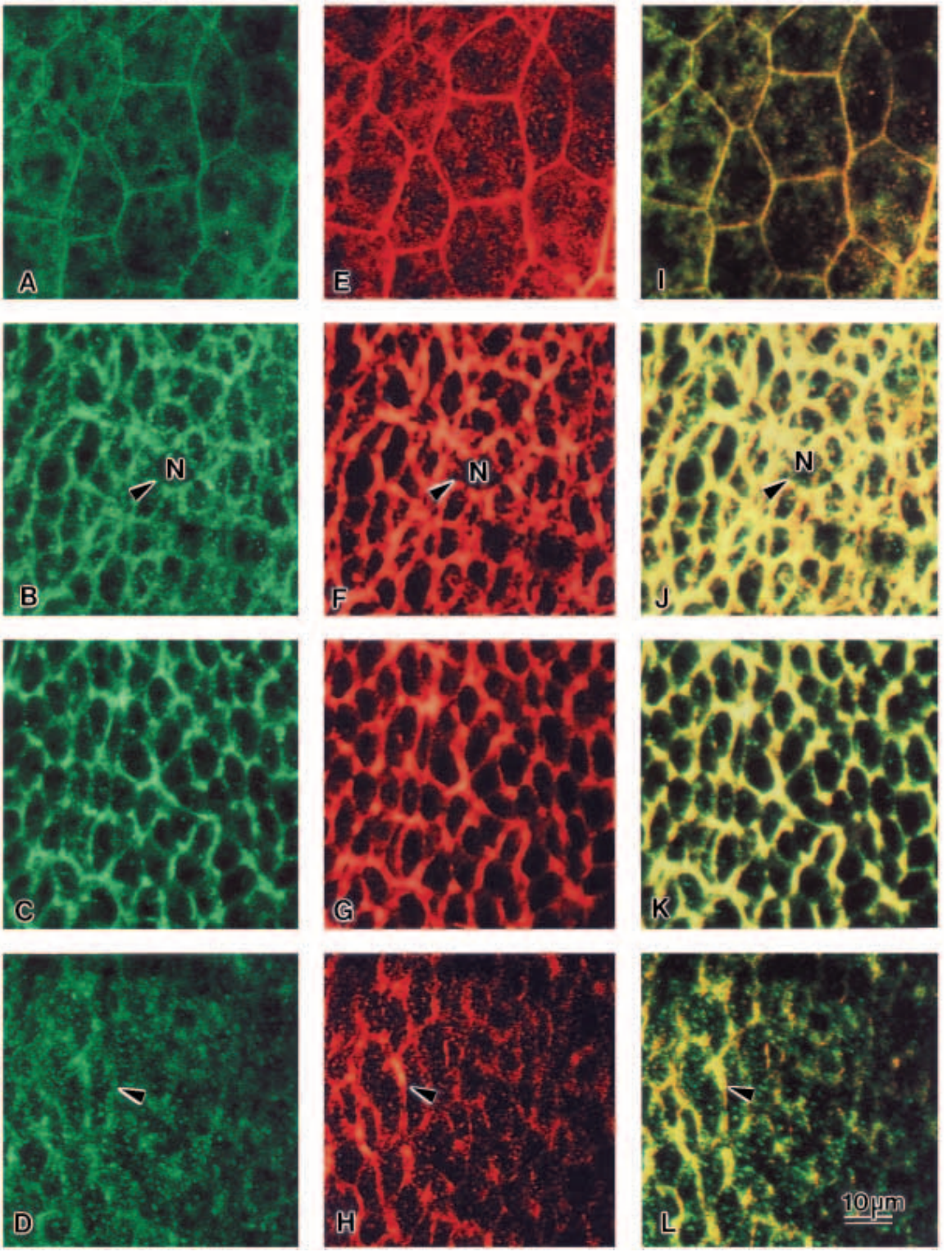

Fig. 2. Actin stained with an anti-actin antibody (C4, A-D) and phalloidin (E-H) shows a similar distribution. CLSM en face micrographs of optical sections through corneal epithelium obtained after double labeling the cells with an anti-actin antibody and phalloidin. The *z* series was obtained for each fluorescent signal, then the images from the same optical plane were merged (I-L). The antibody, C4, stains both the globular (G) and filamentous (F) actin, whereas the phalloidin stains F-actin. Actin at the optical plane of the periderm cells (A,E and I) shows positive staining in the microvilli and as a network surrounding the nucleus. At the optical plane of the periderm-basal cell interface another actin network is present (arrowhead, B,F and J). Note the nearly complete overlap of these two actin-labeling methods, except that the C4 (A-D) has a more punctate appearance in the cytoplasm of the cells. The nuclei (N) do not stain with either method. The optical sections in the center of the basal cells show relatively little staining, but do define the cell borders (C,G,K). In the basal compartment below the nuclear level, the actin is organized into bundles (arrowhead, D,H, L) which appear to be the actin cortical mat described previously with TEM methods. Bar, 10 µm.

embryonic cornea range from 15 to 20 μm in height, and 5 to 10 μm in diameter, depending on the level of the optical section. There are approximately four basal cells beneath each periderm cell (Svoboda, 1992). The ER in the periderm cells appears to form a reticular network (Svoboda, 1991). These characteristics have been established with TEM and confocal analysis (Hay and Revel, 1969; Sugrue and Hay, 1981, 1982; Svoboda and Hay, 1987; Hayashi et al., 1988; Hay and Svoboda, 1989; Svoboda, 1991, 1992) and are illustrated in the drawing (Fig. 1).

F- and G-actin distribution in embryonic corneal epithelia

The organization of the phalloidin-stained F-actin cytoskeleton has been previously described (Svoboda, 1992). However, to aid in the continuity of this paper, it will be briefly described and compared with the distribution of the antigenic sites detected with an anti-actin antibody, C4. The antibody used for this study (C4) binds to all known vertebrate isoforms of actin in both the globular and filamentous configurations (Lessard, 1988). The optical sections of tissue stained with C4 (Fig. 2A-D) have a similar staining pattern to the phalloidin-stained epithelia (Fig. 2E-H) but show more cytoplasmic staining, indicating the distribution of the G-actin in this tissue. The overlap of staining was extensive (Fig. 2I-L) in the periderm and basal cells. The cell borders were easily delineated with both procedures (Fig. 2). Fig. 1 shows the four horizontal planes documenting the actin distribution in the periderm cells (Fig. 2A,E and I), the periderm-basal cell junction (Fig. 2B,F and J), the center of the basal cells, (Fig. 2C,G and K) and the basal compartment of the basal cells (Fig. 2D, H and L). Each cornea is isolated with some surrounding ectoderm. Therefore, an area in the center of the epithelium is selected for confocal scanning. Because the corneas are not perfectly flat, the cells may appear to be in different focal planes. In these en face views of the whole epithelium, the actin is viewed in the microvilli of the periderm cells in the first images (Fig. 2A,E and I) using both detection methods. The merged image (Fig. 2I) shows a nearly complete overlap of signal between actin antibody and phalloidin. At the junction of the periderm and the basal cell layers, another extensive actin network is demonstrated (Fig. 2B,F and J). The actin at this optical plane appears to be mostly F-actin, since there is a large overlap in the detectable signal (arrowhead Fig. 2J). Since the nucleus (N) is negative for actin staining, the dark areas help delineate the two cell layers of the epithelium. The arrowhead points to one of the many areas of overlapping stain. In the central region of the basal cells the F-actin is limited to the cell membranes in the perinuclear area (Fig. 2C,G and K). In addition, there is some punctate staining with the actin antibody that does not colocalize with the phalloidin-stained F-actin (Fig. 2C,K). Below the basal cell nuclei, the actin forms an extensive network (Fig. 2D,H and L, arrowheads). In addition, abundant G-actin labeled with the actin antibody is present (Fig. 2L). This actin network corresponds to the previously described basal actin cortical mat (Sugrue and Hay, 1981, 1982; Sugrue, 1984; Svoboda, 1992).

Quantitative measurement of β-actin probe hybridization

As previously reported, many in situ hybridization parameters can be determined using isotope-labeled probes (Singer et al., 1986; Svoboda, 1991). We used ^{32}P-labeled human β-actin probes to determine the optimum hybridization concentration, test control probes and test pretreatments on mRNA hybridization levels. The epithelia were isolated and hybridized as described in Materials and Methods, then the incorporation of label in the tissue was determined (Fig. 3). The mean and standard deviation for samples for each treatment group (n=5) were calculated. The human β-actin antisense probe hybridized 8-fold greater counts per minute/epithelia than human β-actin sense probe, rat actin probe and RNase-pretreated tissue. In addition, control blank filters contained 16-fold less counts per minute/epithelia than the human β-actin antisense probe (Fig. 3). The tissue is placed on filters, so these controls show the amount of probe that sticks nonspecifically to the filter. In a separate set of experiments it was determined that 65-100 ng of β-actin 40mer oligonucleotide/hybridization was sufficient for hybridization studies.

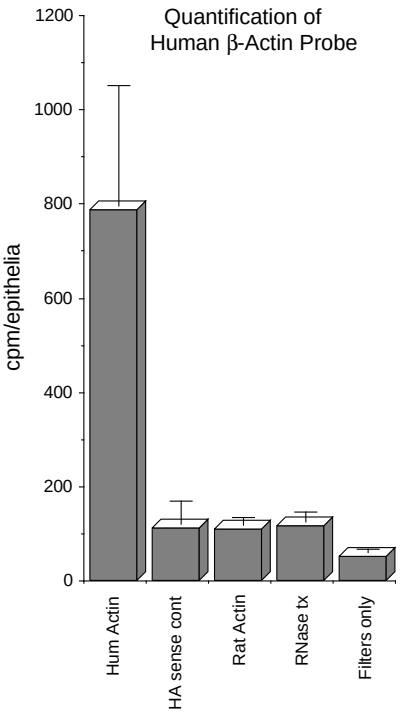

Fig. 3. Quantitative analysis of β-actin in situ hybridization. As reported previously, many in situ hybridization parameters can be determined using isotope-labeled probes (Singer et al., 1986; Svoboda, 1991). Human β-actin probes were used to determine the optimum hybridization conditions and to test various controls. The whole-mount epithelial sheets were hybridized (n=5/group) to ^{32}P-labeled probes using hybridization protocol. The probes used for this study were: human β-actin antisense and sense oligonucleotide (40mer) probes; rat antisense β-actin oligonucleotide (40mer). The human β-actin complementary to mRNA hybridized over 7-fold higher than the sense strand, rat β-actin probe or the RNase-treated tissue. The blank filters hybridized to less probe showing the background of the hybridization procedure.

Intracellular localization of β-actin mRNA

To visualize the intracellular localization of β-actin mRNAs in whole-mount corneal epithelia, biotin-labeled probes were

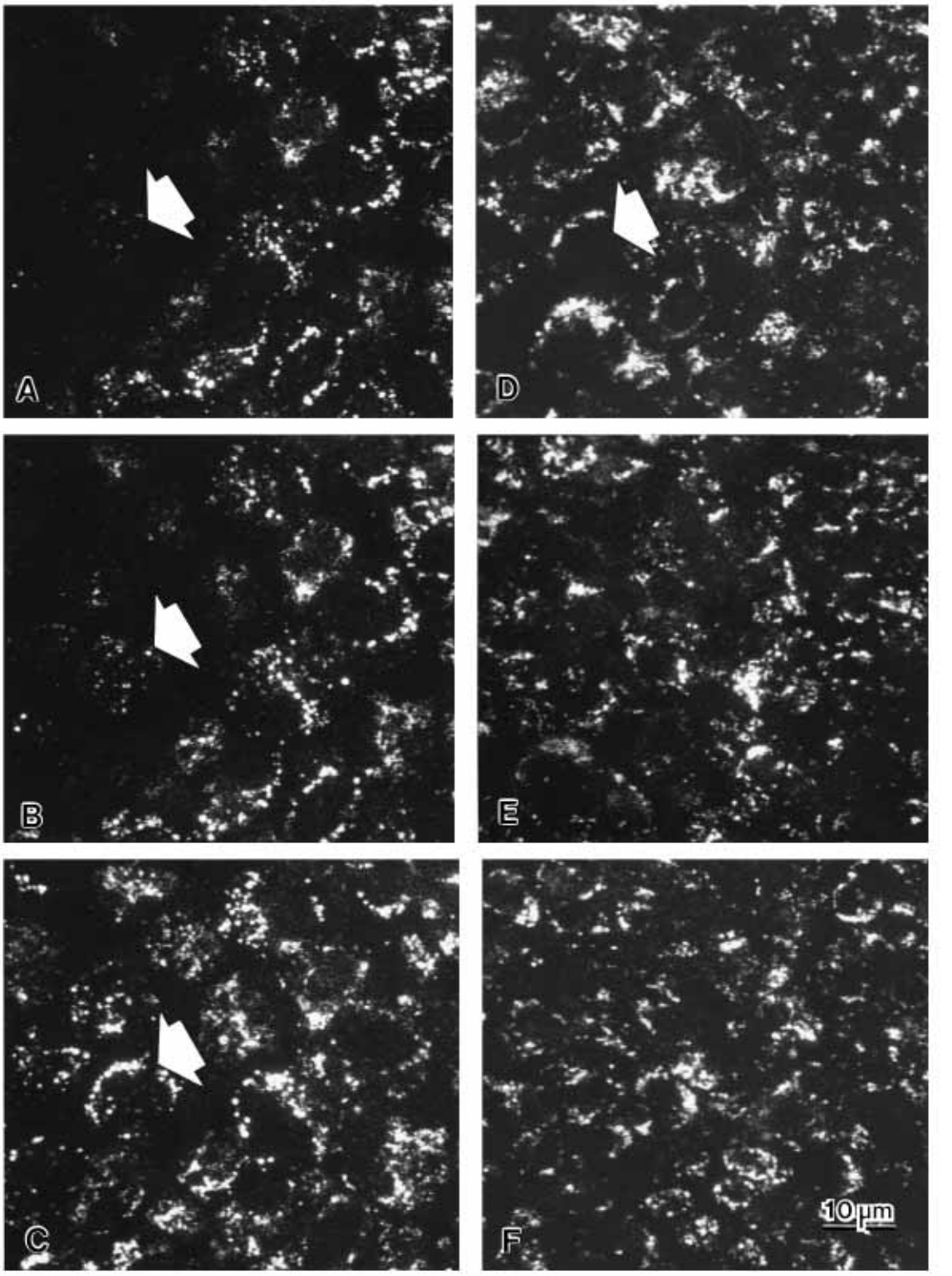

Fig. 4. β-Actin mRNA distribution in corneal epithelia is related to actin protein distribution using FISH analysis. These CLSM micrographs are en face optical sections of actin mRNA after in situ hybridization. The optical section levels are illustrated in the drawing (Fig. 5). (A-D) Periderm: (A) is through the uppermost periderm layer of a corneal epithelium. The tissue is not flat, therefore the right half of the micrograph is lower than the left. The nuclei do not stain and can be used to orient the tissue. The actin mRNA appears to have a polar distribution in this tissue. The cells stain positively directly under the microvilli (arrow, A-D), and in a punctate pattern similar to the cell

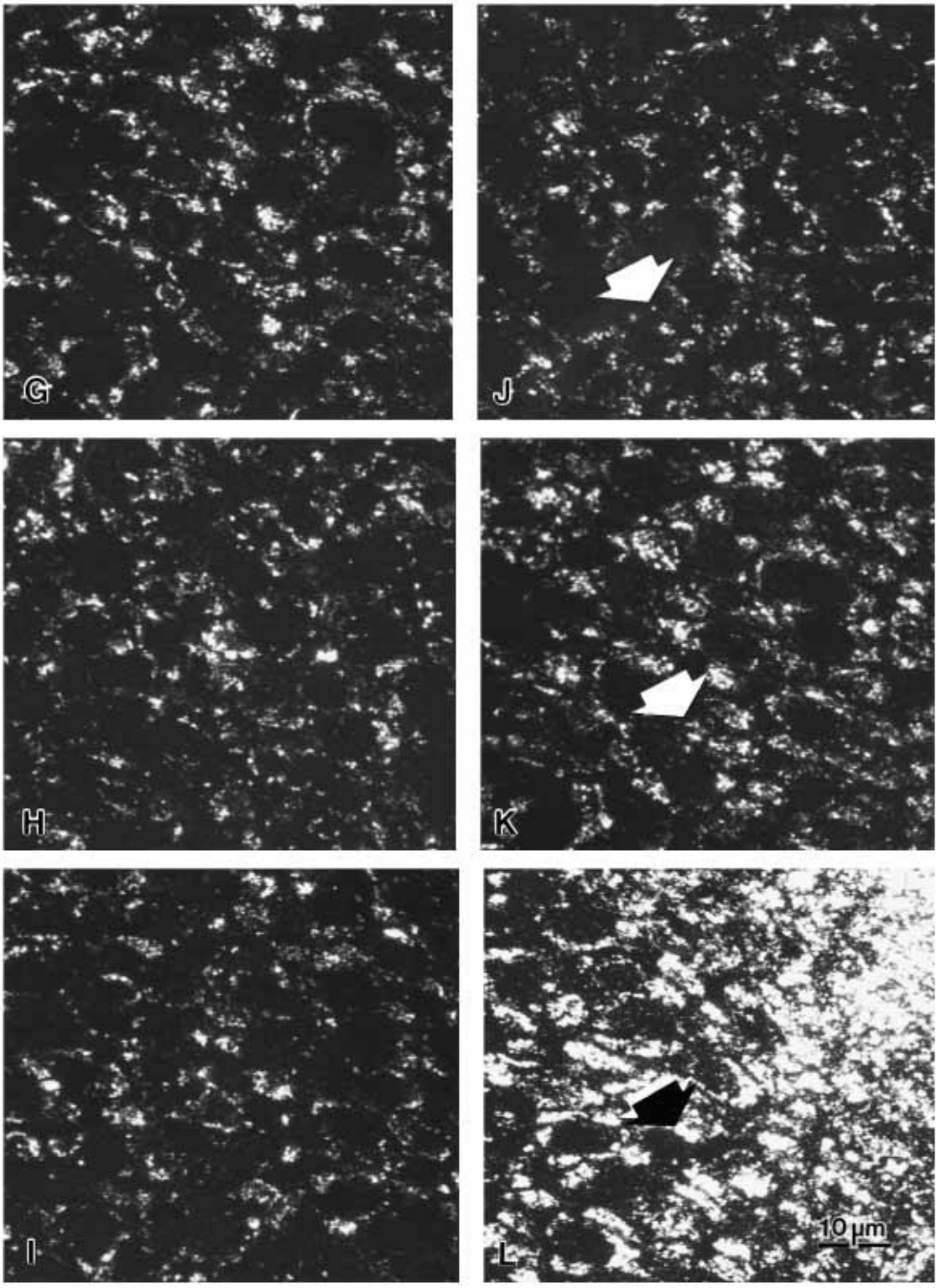

membrane stained with phalloidin. (E,F) Periderm-basal cell transition. CLSM micrographs are en face optical sections of actin mRNA in the optical plane through the periderm-basal cell transition zone. The left portion of these micrographs is in the lower regions of the periderm cells, and the right lower corner is in the upper areas of the basal cells. (G-L) Basal cells. In the central region of the basal cells (G-K) the actin mRNA is closely associated with the cell membrane in a punctate pattern (white arrows, J,K). Below the nuclei of the basal cells (L) the actin mRNA signal becomes more intense (black arrow). This is the region of the actin cortical mat. N, nucleus. Bars, 10 μm.

used. As described in Materials and Methods, both sense and antisense oligonucleotide probes were used. The distribution of actin mRNA was recorded with single label in situ hybridization study. A complete *z*-series taken on a Leica confocal microscope was recorded from separate epithelia that had been hybridized to biotin-labeled probes specific for the sense or antisense β-actin mRNA. The biotin-labeled probes were detected with FITC-avidin. This adds an addtional step to the procedure described above. Since it is difficult to quantitate fluorescent data, we are using this procedure just to visualize the intracellular distribution of the probe-labeled mRNA. The optical sections in the complete *z*-series were taken 1 μm apart. Selected micrographs are shown (Fig. 4). The accompanying diagram illustrates the level of each optical section in these plates (Fig. 5). The actin mRNA is distributed throughout both the periderm and basal cell layers in a punctate pattern similar to the actin staining pattern. The β-actin mRNA first appeared in the periderm cells just beneath the position of the microvilli (Fig. 4A-B, white arrows). The β-actin mRNA also appeared as a punctate pattern near the cell membranes in the periderm cells (Fig. 4C-D, white arrows). The central regions of the cells did not hybridize to the actin olgionucleotide probe, therefore leaving large negative areas. In independent studies, it has been shown that these areas contain the RER and nuclei of the periderm cells (Svoboda, 1991). At the periderm-basal cell junction area (Fig. 4E-F) the actin mRNA is abundant and also appears to be near the area of cell membranes (compare Fig. 2B,F and J, to Fig. 4E and F). In the central region of the basal cells the staining pattern appears mainly in the cell membrane area (Fig. 4G-K, arrow), similar to the F-actin protein distribution (Fig. 2C,G and K; Fig. 4G-K, arrows, J,K). Below the basal cell nuclei, the β-actin mRNA increases and appears to have a punctate pattern throughout the cytoplasm (Fig. 4L, black arrow). This indicates that the β-actin mRNA and the actin cortical mat (Fig. 2D,H and L) are both occupying the cytoplasm immediately above the basal plasma membrane.

The apical-basal distribution pattern was determined by taking the complete *z*-series file (21 images), reconstructing a three-dimensional composite, then imaging a slice at 90°. This created a *xz* image of the same data files (Fig. 6A-D) shown in Fig. 2A-D and Fig. 4, respectively. These images clearly show the outlines of cell membranes that correlate with a *xz* image from a corneal epithelia stained for actin protein (Fig. 6A) and β-actin mRNA (Fig. 6D). The anti-actin antibody-labeled both periderm cells (Fig. 6A, arrowhead) and lateral cell membranes (Fig. 6A, arrow). As stated previously, the nuclei (N) do not stain with either the anti-actin antibody or phalloidin. The β-actin mRNA was also found in the periderm cells near the apical surface (Fig. 6D, arrowhead) and along lateral cell membranes (Fig. 6D, arrow). In addition, actin mRNA appeared in the basal area below nuclei (N).

Immunohistochemistry and in situ hybridization controls had minimal background signal (Fig. 6B,E and F). In addition to secondary antibody controls (Fig. 6B), it was necessary to demonstrate FITC fluorescent probes were not recorded onto the rhodamine photomultiplyer tube. Therefore, we routinely had single-labeled material for each fluorescent tag scanned at the same confocal microscope settings with the opposite filter set and photomultiplyer tube. These samples were termed 'cross-over' controls. The cross-over and secondary antibody controls were negative for the immunohistochemical studies (Fig. 6B and C).

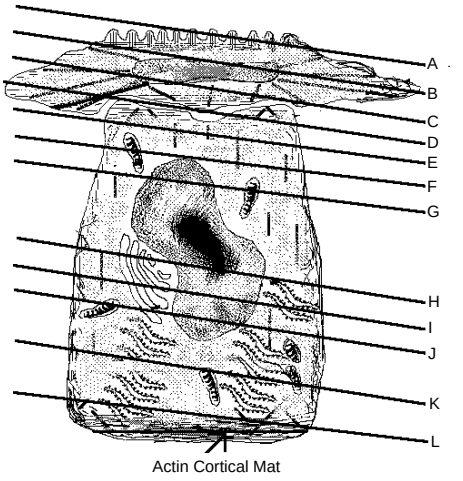

Fig. 5. This schematic drawing of the corneal epithelial cells shows the level of the 12 optical planes that correspond to the micrographs in Fig. 4.

As described for the isotopic probes, the biotin-avidin FITC-labeled tissues also had companion controls. The no probe and β-actin sense oligonucleotide controls were negative when compared to β-actin antisense tissue at the same voltage, offset and pinhole settings of the confocal microscope (Fig. 6E and F). RNase-pretreated tissue was also negative when viewed at the same confocal settings (data not shown).

In conclusion, the isotopic quantitative data indicate that the β-actin mRNA is abundant in the corneal epithelial cells and the biotin-avidin FITC-labeled probes demonstrate that the distribuion of the β-actin mRNA is polarized. In addition, the general intracellular distribution of the β-actin mRNA appears to correlate well with F-actin. In future experiments we plan to combine immunohistochemistry with in situ hybridization to definitively show the relationship between F-actin and its mRNA.

DISCUSSION

These experiments are the first demonstration that β-actin mRNA is polarized in embryonic corneal epithelia. In addition the β-actin mRNA and the F-actin appear to have the same distribution in intact corneal epithelium. These studies extend previous experiments (Svoboda, 1992) that show that F-actin staining delineates the cell borders and microvilli of periderm cells in the most apical optical sections of embryonic cornea. The double-labeling experiments show that G and F-actin were recognized by the C4 antibody, and that phalloidin overlapped this staining in the microvilli, cell periphery and actin cortical mat. However, the G-actin stained only by the C4 antibody has a cytoplasmic distribution in both the periderm and basal cells. G-actin is also present in the actin cortical mat area below the basal cell nuclei. At the level of the basal cell nucleus, F-actin is sparse, only associated with the lateral cell membranes, but G-actin could be detected in the cytoplasm. At the optical plane below the nuclei, the actin forms an elaborate actin cortical mat.

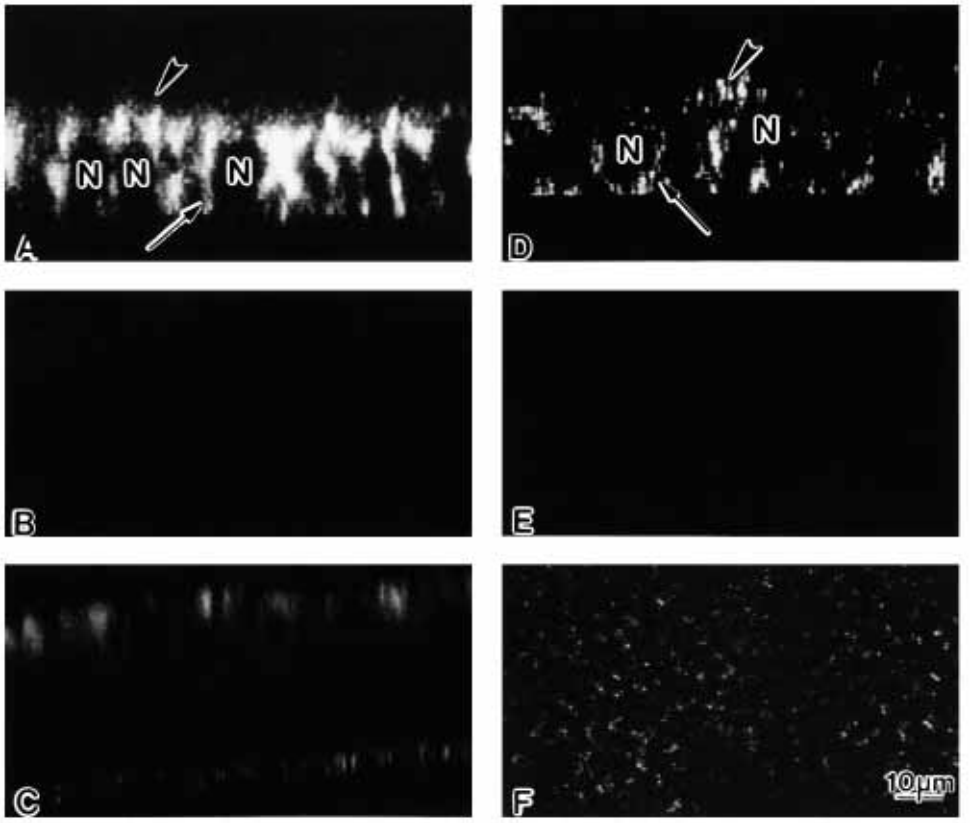

Fig. 6. Apical-basal polarity of actin and actin mRNA with controls. The complete data files from epithelia stained with anti-actin antibody (A) or β-actin mRNA (D) were used to produce a three-dimensional image for each file. The stack of images was viewed at a 90° angle, to see a 'cross-sectional' area of the tissue. (A) The actin protein viewed from the same file as Fig. 2A-D was used to produce this slice of the 3-D reconstruction. Actin protein is prominent in the periderm apical membrane (arrowhead) and along the lateral membranes of the basal cells (arrow). The nuclei (N) do not label with either the antibody or β-actin probe. (B) Secondary antibody control: corneal epithelial tissue was used to test the distribution of goat anti-mouse FITC-labeled antibody without the primary antibody. The tissue was scanned at the same pinhole, voltage and offset as positive tissue. (C) Cross-over control: single-labeled FITC samples were viewed on the rhodamine channel at the settings for recording rhodamine signal. The amount of signal that was recored on the rhodamine channel was termed cross-over. (D) β-Actin mRNA viewed in an *xz* focal plane from the same file shown in Fig. 4. The β-actin antisense probe labeled the periderm cells (arrowhead), lateral cell membrane area (arrow) and beneath the nuclei (N) in the basement membrane zone. (E) β-Actin sense control: this *xy* image of the β-actin sense control showed minimal background staining at the confocal settings used to record the file shown in Fig. 4. (F) No probe control: this *xy* image of a tissue sample that did not contain the biotin-labeled probe, and was only reacted with the secondary signal avidin, shows the amount of endogenous biotin that may interfere with the biotin-avidin labeling protocol.

Beta-actin mRNA staining is visualized as discrete punctate areas. The mRNA is positive at the optical plane just below the periderm cell apical membrane surface, similar to actin protein found in microvilli. These cells also contain punctate staining near the cell membranes and in the periderm-basal cell junction area. At the level of the basal cell nucleus the actin mRNA is present in a punctate pattern in a cell membrane distribution pattern. Below the basal cell nuclei the actin mRNA staining increases at the level of the actin cortical mat. The actin mRNA has a distinct pattern in corneal epithelia that is similar to the F-actin protein distribution but differs from the RER-associated collagen mRNA distribution (Svoboda, 1991).

The actin antibody (C4) used for this study recognizes a conserved epitope that reacts with all six known vertebrate isoactins, *Dictyostelium discoidem* and *Physarum polycephalum* (Lessard, 1988). Although the antibody does not block actin polymerization, it does bind to G-actin (Lessard, 1988). The staining pattern reported here confirms that the antibody binds to both F and G forms of actin, since it colocalized with phalloidin staining and had a punctate cytoplasmic distribution.

The whole actin gene is a highly conserved structure and exon 2 has 80-100% homology (Nakajima-Iijima et al., 1985). Due to this sequence homology between species, cross-hybridization will occur with most actin probes (Ponte et al., 1983). The β-actin probe used in this study was a 40-base single-stranded oligonucleotide (62.5% GC content) from exon 2 of the human actin gene (Nakajima-Iijima et al., 1985). Because this region of the actin gene is highly conserved it was not surprising that the human probe reacted with chicken tissue. However, it was surprising that the rat actin probe did not work on our chick tissue, since the homology between the regions should be similar. The rat actin probe worked well in rat tissue; therefore, we know that the oligonucleotide was intact after labeling. In contrast, the actin probe used in previous studies was a larger cDNA fragment that was labeled by nick translation (Singer et al., 1986).

Although the probes were to different regions of the actin mRNA, our study confirms and extends previous work that showed actin mRNA has a polarized distribution in cultured cells. The actin mRNA was found at the leading lamellapodia of cultured fibroblasts, myoblasts (Singer et al., 1986) and microvascular pericytes (Hoock et al., 1991). The lamellapodia have been shown to be the area of active actin synthesis in mobile cultured cells (Wang, 1984).

The embryonic corneal epithelium is not moving, but does have a polarized actin protein distribution (Svoboda, 1992). Intestinal epithelial cells also have a polarized actin-rich apical brush border. Cheng and Bjerknes (1989) demonstrated that the β-actin mRNA was enriched in the apical area of the tissue. This laboratory used sectioned material for both F-actin and β-actin mRNA distribution. The probes were ^{35}S-labeled and

densitometry methods were used to determine the distribution of actin mRNA. The current study contributes a more detailed intracellular distribution of F- and G-actin protein and β-actin mRNA than the use of sectioned intestinal epithelia (Cheng and Bjerknes, 1989). Since the biotin-labeled probes need the additional detection steps involving fluorescence and confocal microsopy, a direct quantitative comparison between the isotopic and nonisotopic preparations would not be valid. The individual fluorescent images could be evaluated for total fluorescence intensity, but that was not the intention of this study. We wanted to determine the spatial distribution of the mRNA, not the exact amount present. Combining fluorescent probes with confocal microsopy allows the examination of intracellular ligand distribution. Furthermore, producing three-dimensional images from the two-dimensional data sets allows the examination of the fluorescent markers from different angles (Fig. 6A and D).

Although this study does not address the question of how the actin mRNA was translocated to these intracellular sites, other researchers have determined that the translocation of actin mRNA to lamellapodia of cultured cells depends on actin microfilaments (Sundell and Singer, 1991). In acidian oocytes, actin mRNA and poly(A)$^+$ RNA were localized to the cytoskeletal framework of embryos by hybridization, but the histone mRNA was distributed throughout the eggs (Jeffery and Meier, 1983). In another embryonic system, Melton's group has cloned several mRNAs that were preferentially localized to the animal or vegetal pole of mature *Xenopus* eggs (Mowry and Melton, 1992; Yisraeli et al., 1990). One of these mRNAs, vg-1, was localized to the vegetal pole by a transporting process that required microtubules and an anchoring mechanism that requires actin (Yisraeli et al., 1990). It was further found that 340 nucleotides of the 3′ untranslated region of the mRNA were responsible for the translocation and anchoring mechanism (Mowry and Melton, 1992). These types of mechanisms may also be operating in the differentiated epithelial cells.

Our future experiments will address some of these translocation questions and others such as: are the mRNAs stored in these locations or actively translated? What is the three-dimensional relationship between actin and actin mRNA?

We thank Daniel Orlow, Melina Fan, Michelle Hirsch and Cromwell Schubarth for their technical and photographic assistance. We thank Dr Carl Franzblau, the Associate Dean for Graduate Biomedical Sciences, for his assistance in establishing the Leica Confocal Facilities at Boston University School of Medicine. We thank Dr James Lessard for his generous antibody gift (anti-actin) and for reviewing the manuscript. This work was supported by a grant from NIH (RO1 EY-08886).

REFERENCES

Adams, A., Fey, E. G., Pike, S. F., Taylorson, C. J., White, H. A. and Rabin, B. R. (1983). Preparation and properties of a complex from rat liver of polyribosomes with components of the cytoskeleton. *Biochem. J.* **216**, 215-226.

Batten, B. E., Aalberg, J. J. and Anderson, E. (1980). The cytoplasmic filamentous network in cultured ovarian granulosa cells. *Cell* **44**, 885-895.

Ben-Ze'ev, A., Duerr, A., Solomon, F. and Penman, S. (1979). The outer boundary of the cytoskeleton: A lamina derived from plasma membrane proteins. *Cell* **17**, 859-865.

Cheng, H. and Bjerknes, M. (1989). Asymmetric distribution of actin mRNA and cytoskeletal pattern generation in polarized epithelial cells. *J. Mol. Biol.* **210**, 541-549.

Hay, E. D. and Revel, J. P. (1969). Fine structure of the Developing Avian Cornea. *Monographs in Developmental Biology* (ed. A. Wolsky and P. S. Chen). S. Karger A.G., Basel.

Hay, E. D. and Svoboda, K. K. H. (1989). Extracellular matrix interaction with the cytoskeleton. In *Cell Shape, Determinant, Regulation and Regulatory Role* (ed. W. D. Stein and F. Bronner), pp. 147-172. Academic Press, New York.

Hayashi, M., Ninomiya, Y., Hayashi, K., Linsenmayer, T. F., Olsen, B. R. and Trelstad, R. L. (1988). Secretion of collagen types I and II by epithelial and endothelial cells in the developing chick cornea demonstrated by in situ hybridization and immunohistochemistry. *Development* **103**, 27-36.

Hoock, T. C., Newcomb, P. M. and Herman, I. M. (1991). Beta actin and its mRNA are localized at the plasma membrane and the regions of the moving cytoplasm during cellular response to injury. *J. Cell Biol.* **112**, 653-664.

Jeffery, W. R. and Meier, S. (1983). A yellow crescent cytoskeletal domain in Ascidian eggs and its role in early development. *Dev. Biol.* **96**, 125-143.

Lawrence, J. B. and Singer, R. H. (1986). Intracellular localization of messenger RNA for cytoskeletal proteins. *Cell* **45**, 407-415.

Lenk, R., Ransom, L., Kaufmann, Y. and Penman, S. (1977). A cytoskeletal structure with associated polyribosomes obtained from HeLa cells. *Cell* **10**, 67-78.

Lenk, R. and Penman, S. (1979). The cytoskeletal framework and poliovirus metabolism. *Cell* **16**, 289-301.

Lessard, J. L. (1988). Two monoclonal antibodies to actin, One muscle selective and one generally reactive. *Cell Motil. Cytoskel.* **10**, 349-362.

Meier, S. and Hay, E. D. (1973). Synthesis of sulfated glycosaminoglycans by embryonic corneal epithelium. *Dev. Biol.* **35**, 318-331.

Mowry, K. L. and Melton, D. A. (1992). Vegetal messenger RNA localization directed by a 340-nt RNA sequence element in Xenopus oocytes. *Science* **255**, 991-994.

Nakajima-Iijima, S., Hamada, H., Reddy, P. and Kakunaga, T. (1985). Molecular structure of the human cytoplasmic β-actin gene: Interspecies homology of sequences in the introns. *Proc. Nat. Acad. Sci. USA* **82**, 6133-6137.

Pawley, J. B. (1990). Fundamental limits in confocal microscopy In *Handbook of Biological Confocal Microscopy* (ed. J. B. Pawley), pp. 15-26.

Ponte, P., Gunning, P., Blau, H. and Kedes, L. (1983). Human actin genes are single copy for α-skeletal and α-cardiac actin but multicopy for β- and γ-cytoskeletal genes: 3′ untranslated regions are isotype specific but are conserved in evolution. *Mol. Cell. Biol.* **3**, 1783-1791.

Quaranta, V. and Jones, J. C. R. (1991). The internal affairs of an integrin. *Trends Cell Biol.* **1**, 2-4.

Ramaekers, F. C. S., Bennedetti, E. L., Dunia, I., Vorstenbosch, P. and Bloemendal, H. (1983). Polyribosomes associated with microfilaments in cultured lens cells. *Biochim. Biophys.* **740**, 441-448.

Schliwa, M. (1981). Proteins associated with cytoplasmic actin. *Cell* **25**, 587-590.

Schliwa, M. (1982). Action of cytochalasin D on cytoskeletal networks. *J. Cell Biol.* **92**, 79-91.

Singer, R. H., Lawrence, J. B. and Villnave, C. (1986). Optimization of in situ hybridization using isotopic and non-isotopic detection methods. *BioTechniqes* **4**(3), 230-250.

Singer, R. H., Langevin, G. L. and Lawrence, J. B. (1989). Ultrastructural visualization of cytoskeletal mRNAs and their associated proteins using double-label in situ hybridization. *J. Cell Biol.* **108**(6), 2343-2353.

Stepp, M. A., Spurr-Michaud, S. and Gipson, I. K. (1993). Integrins in the wounded and unwounded stratified squamous epithelium of the cornea. *Invest. Ophthalmol. Vis. Sci.* **34**, 1829-1844.

Sugrue, S. P. (1984). The interaction of extracellular matrix with the basal cell surface of embryonic corneal epithelia. In *Matrices and Cell Differentiation*, pp. 77-87. New York, NY: Alan R. Liss, Inc.

Sugrue, S. P. (1987). Isolation of collagen binding proteins from embryonic chicken corneal epithelial cells. *J. Biol. Chem.* **262**, 3338-3343.

Sugrue, S. P. (1988). Identification and immunolocalization of the laminin binding protein from embryonic avian corneal epithelial cells. *Differentiation* **38**, 169-176.

Sugrue, S. P. and Hay, E. D. (1981). Response of basal epithelial cell surface and cytoskeleton to solubilized extracellular matrix molecules. *J. Cell Biol.* **91**, 45-54.

Sugrue, S. P. and Hay, E. D. (1982). Interaction of embryonic corneal epithelium with exogenous collagen, laminin, and fibronectin: role of endogenous protein synthesis. *Dev. Biol.* **92**, 97-106.

Sugrue, S. P. and Hay, E. D. (1986). The identification of extracellular matrix (ECM) binding sites on the basal surface of embryonic corneal epithelium and the effect of ECM binding on epithelial collagen production. *J. Cell Biol.* **102**, 1907-1916.

Sundell, C. L. and Singer, R. H. (1990). Actin mRNA localizes in the absence of protein synthesis. *J. Cell Biol.* **111**, 2397-2403.

Sundell, C. L. and Singer, R. H. (1991). Requirement of microfilaments in sorting of actin messenger RNA. *Science* **253**, 1275-1277.

Svoboda, K. K. H. and Hay, E. D. (1987). Embryonic corneal epithelial interaction with exogenous laminin and basal lamina is F-actin dependent. *Dev. Biol.* **123**, 455-469.

Svoboda, K. K. H. (1991). Intracellular localization of types I and II collagen mRNA and endoplasmic reticulum in embryonic corneal epithelia. *J. Cell Sci.* **100,** 23-33.

Svoboda, K. K. H. (1992). Embryonic corneal epithelial actin alters distribution in response to laminin. *Invest. Ophthalmol. Vis. Sci.* **33**, 324-333.

Taneja, K. L., Lifshitz, L. M., Fay, F. S. and Singer, R. H. (1992). Poly(A) RNA codistribution with microfilaments: Evaluation by in situ hybridization and quantitative digital imaging microscopy. *J. Cell Biol.* **119**, 1245-1260.

Wang, Y. L. (1984). Reorganization of actin filament bundles in living fibroblasts. *J. Cell Biol.* **99**, 1478-1485.

Wilson, T. (1990). The role of the pinhole in confocal imaging systems. In *Handbook of Biological Confocal Microscopy* (ed. J. B. Pawley), pp. 113-126.

Wolosewick, J. J. and Porter, K. R. (1976). Stereo high-voltage electron microscopy of whole cells of the human diploid line, WI-38. *Amer. J. Anat.* **147**, 303-324.

Wolosewick, J. J. and Porter, K. R. (1979). Microtrabecular lattice of the cytoplasmic ground substance, artifact or reality? *J. Cell Biol.* **82**, 114-139.

Yisraeli, J. K., Sokol, S. and Melton, D. A. (1990). A two-step model for the localization of maternal mRNA in Xenopus oocytes: Involvement of microtubules and microfilaments in the translocation and anchoring of Vg1 mRNA. *Development* **108**, 289-298.

(Received 16 June, 1993 - Accepted, in revised form 28 September, 1993)